

Preparation and Characterization of Lithium Niobate Single Crystals Doped with Zinc and Erbium

S. M. Masloboeva^a, *, I. N. Efremov^a, I. V. Biryukova^a, N. A. Teplyakova^a, and M. N. Palatnikov^a

^a *Tananaev Institute of Chemistry and Technology of Rare Elements and Minerals (separate subdivision), Kola Scientific Center (Federal Research Center), Russian Academy of Sciences, Apatity, Murmansk oblast, 184209 Russia*

**e-mail: sofia_masloboeva@mail.ru*

Received December 22, 2020; revised February 20, 2021; accepted March 1, 2021

Abstract—This paper reports a process for the growth of zinc–erbium codoped lithium niobate single crystals using a growth charge synthesized from a $\text{Nb}_2\text{O}_5\text{:Zn:Er}$ precursor and Li_2CO_3 . Characterization of the $\text{LiNbO}_3\text{:Zn:Er}$ crystals by high-speed evaluation of the number of scattering centers, piezoacoustic measurements, photoinduced light scattering, and laser conoscopy has demonstrated that they have high optical quality. The proposed technological approaches are aimed at designing functional materials with fundamentally new characteristics for electronics, acoustoelectronics, and integrated, quantum, and laser optics.

Keywords: lithium niobate single crystal, doping, microdefect density, piezoelectric modulus, photoinduced light scattering, laser conoscopy

DOI: 10.1134/S0020168521070116

INTRODUCTION

Lithium niobate (LiNbO_3) is one of the most important ferroelectric, nonlinear optical, pyroelectric, and piezoelectric materials [1–4]. Doping of LiNbO_3 with various elements (rare earths, alkaline-earth and transition metal, and others) makes it possible to significantly modify its properties [5–7] and appreciably extend its application field. The photorefractive effect and photoinduced light scattering are known to cause severe laser beam destruction in lithium niobate crystals and be interfering factors in light generation and conversion by the crystals [8]. For this reason, studies aimed at optimizing the photorefractive properties of LiNbO_3 crystals are of great current interest for designing materials with tailored characteristics.

An important scientific and practical issue is the development of new lithium niobate-based materials codoped with a few impurities. The purpose of such studies is to find effective ways of modifying the structure of crystals in a controlled manner, improving their electro-optical and nonlinear optical properties, and raise their optical damage threshold. The properties of doubly doped LiNbO_3 crystals have been the subject of a rather limited number of studies [9–17], which used crystals grown from charges prepared by solid-state synthesis [18]. However, in such a case optically homogeneous crystals with a sufficiently high dopant concentration are difficult to grow. For obtaining doubly doped LiNbO_3 crystals, a homogeneous doping method proposed previously [19] is of interest.

The functioning of apparatus basic to advanced optoelectronic and telecommunication technologies depends in many respects on lithium niobate crystals. In particular, they are widely used in cellular communication and for ultra-high-speed internet. Crystals for such applications should meet rather stringent requirements for their optical homogeneity and optical damage threshold. Doping of lithium niobate crystals with nonphotorefractive impurities (Zn, Mg, Sc, and others) is known to markedly improve their optical damage threshold. At the same time, $\text{LiNbO}_3\text{:Er}$ crystals are used as materials for optical amplifiers in optical fiber communication systems. Raising the optical damage threshold of such materials by codoping with Zn and Er, yielding $\text{LiNbO}_3\text{:Zn:Er}$ crystals, makes it possible to amplify higher power optical radiation without signal distortion, which accordingly leads to an increase in optical fiber data rate.

The objectives of this work were to develop a process for the growth of optically homogeneous $\text{LiNbO}_3\text{:Zn:Er}$ crystals using a charge synthesized from a $\text{Nb}_2\text{O}_5\text{:Zn:Er}$ precursor and lithium carbonate and study the properties of the crystals using high-speed quality assessment methods, piezoacoustics, photoinduced light scattering (PILS), and laser conoscopy.

EXPERIMENTAL

A $\text{LiNbO}_3\text{:Zn:Er}$ (5.5 mol % Zn and 1.0 wt % Er) charge for Czochralski growth of lithium niobate crys-

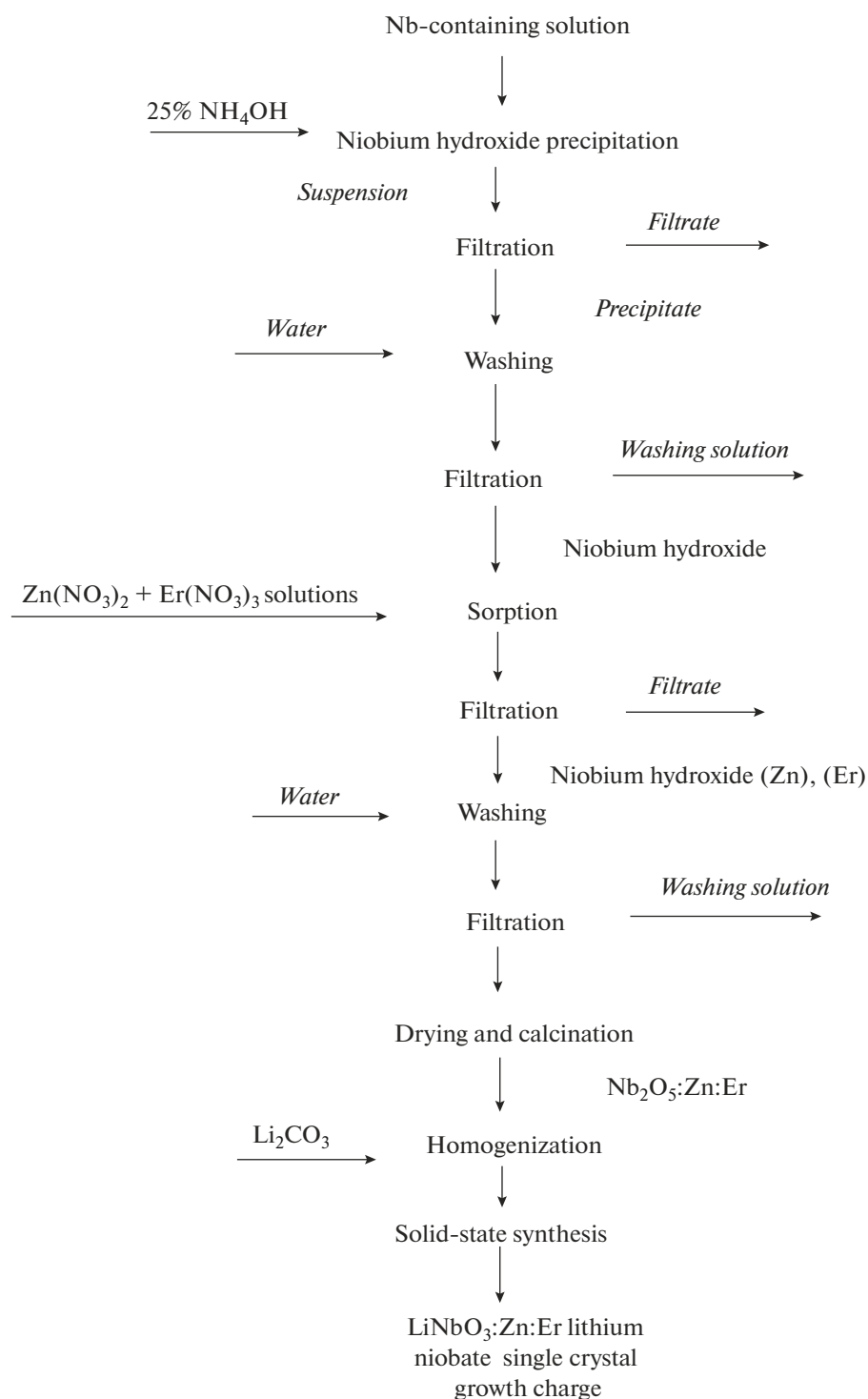


Fig. 1. Flow diagram illustrating the preparation of a single-phase zinc-erbium codoped lithium tantalate crystal growth charge.

tals was synthesized according to the flow diagram shown in Fig. 1.

In our preparations, we used a high-purity niobium-containing solution (142.8 g/L of Nb_2O_5 and 139.7 g/L of F^-) prepared by dissolving Nb_2O_5 (extra-pure grade) in HF (extra-pure grade). High-purity ni-

biom hydroxide was prepared via precipitation with ammonia from the starting solution. The precipitate was washed three times with deionized water at a solid : liquid ratio of 1 : 4. During the precipitation process, the solution was maintained at pH 8 in order to reduce the content of NH_4^+ cations (which react with zinc to

form highly soluble ammonia complexes [20]) in the wet precipitate. After drying at 90°C, the hydroxides (with a relative humidity of ~65%) were mixed with zinc and erbium nitrate solutions of preset concentration. The mixing process was run for 3 h. The precipitate was separated from the solution by filtration, washed once with deionized water at a solid : liquid ratio of 1 : 1.5, dried at 140°C, and calcined at 1000°C for 3 h. A granulated growth charge of congruent composition was synthesized from a prehomogenized mixture of a Nb₂O₅:Zn:Er precursor and Li₂CO₃ (extrapure grade), which was thermally calcined in a compartment furnace at ~1250°C for 5 h. Zn(NO₃)₂ + Er(NO₃)₃ solutions were prepared by dissolving the ZnO (extrapure grade) and Er₂O₃ (extrapure grade) oxides in HNO₃ (extrapure grade).

Dopant (Zn and Er) concentrations in the precursor and growth charge were determined by X-ray fluorescence spectrometry (XFS) on a Spectroscan MAX-GV spectrometer. The quantitative amount of niobium in the starting solution and lithium niobate growth charge (after dissolution) was determined gravimetrically. Fluoride ions were determined potentiometrically using an EV-74 ion-selective meter fitted with an EVL-1M3 F-selective electrode. The LiNbO₃:Zn:Er doped growth charge was analyzed for fluorine by the pyrohydrolysis method. The concentration of cation impurities (Mg, Al, Si, Ca, Ti, V, Cr, Mn, Fe, Co, Ni, Cu, Zr, Ta, Mo, Sn, and Pb) was determined by spectral analysis with a DFS-13 instrument. Li concentration in the LiNbO₃:Zn:Er growth charge was evaluated by inductively coupled plasma atomic emission spectroscopy.

The phase composition of the Nb₂O₅:Zn:Er precursor and LiNbO₃:Zn:Er growth charge was determined by X-ray diffraction on a DRON-2 diffractometer at a continuous scan rate of 2°/min 2θ (CuK_α radiation, graphite monochromator).

LiNbO₃:Zn:Er lithium niobate single crystals were grown in the [001] direction by the Czochralski technique from 80-mm-diameter platinum crucibles in air, using a Kristall-2 induction furnace. Growth conditions of heavily doped lithium niobate crystals were studied by Palatnikov et al. [21], in combination with measurements of the temperature gradient across the solid–liquid interface. Their results [21] made it possible to design a heating unit that ensured an axial temperature gradient of ~3°C/mm near the melt surface and an extended isothermal region with a temperature of 1210°C in the post-growth lithium niobate single crystal annealing zone after the crystal was lifted to a platinum shield. Other crystal growth process parameters were chosen experimentally so as to ensure a flat solidification front. The translation rate was 0.8 mm/h, and the rotation rate was 14 rpm.

To relieve the thermoelastic stress, the crystals were heat-treated at 1240°C for 24 h in a Lantan high-tem-

perature annealing furnace. After that, to determine the dopant concentrations in each crystal, plates were cut from the upper part (cone) and the lower cylindrical part (tail end) of the boule. Erbium was determined by XFS and zinc was determined by atomic absorption spectroscopy on an Analyst 400 spectrometer. The rest of the boule was converted into a single-domain state via high-temperature electrodiffusion annealing by applying a direct current during cooling of the samples in the temperature range from 1241 to 800°C.

The optical quality of the grown crystals was quantified by the number of scattering centers. Conversion of the crystals into a single-domain state and their piezoelectric modulus d_{333} were evaluated by techniques and with equipment described elsewhere [22].

In our PILS experiments, we used an MLL-100 yttrium aluminum garnet laser emitting at 514.5 nm. A sample to be studied was placed in the path of the laser beam so that the wave vector of the light wave was directed along its *Y* axis, that is, along the normal to the input crystal face, and the electric field vector *E* of the light wave was parallel to the *z* axis of the sample, that is, to the polar axis of the lithium niobate crystal (*P*_s). In this scattering geometry, the photorefractive effect in LiNbO₃ crystals shows up most clearly. To obtain large conoscopic patterns, we used a laser conoscopy method [23, 24] (MLL-100 laser, λ = 514.4 nm, *P* = 1 or 90 mW). In our conoscopy experiments, a crystalline sample was placed on a two-axis optical translation stage, which allowed us to scan the entire input face of the sample by the laser beam and obtain numerous conoscopic patterns corresponding to different areas in a cross section of the sample under investigation.

RESULTS AND DISCUSSION

Preliminary results demonstrate that, to obtain a lithium niobate growth charge with a predetermined Zn dopant concentration, a 3% excess of Zn with respect to its nominal amount is needed. Analysis of our experimental data on the Zn (Er) content of LiNbO₃ growth charges showed that, to within admissible uncertainty of the analytical technique used by us, the Zn (Er) dopant passed almost quantitatively from the zinc (erbium) nitrate solutions to the Nb₂O₅:Zn:Er precursor and that the Zn content of the LiNbO₃:Zn:Er corresponded to the intended one (Table 1).

X-ray diffraction results indicated that, at the dopant concentrations used by us, the Nb₂O₅:Zn:Er precursor was not single-phase. The X-ray diffraction pattern of the sample calcined at 1000°C for 3 h, has a sharp peak at 2.95 Å, corresponding to the ZnNb₂O₆ phase [25]. The other reflections are attributable to Nb₂O₅ as a major phase. At the same time, analytical data indicate that the LiNbO₃:Zn:Er lithium niobate growth charge consists of single-phase material corresponding to LiNbO₃ [26].

Table 1. Zinc and erbium concentrations in the $\text{Nb}_2\text{O}_5\text{:Zn:Er}$ precursor and $\text{LiNbO}_3\text{:Zn:Er}$ growth charge (intended Zn and Er concentrations in the growth charge: 2.44 and 1.0 wt %, respectively)

Weight percent in the $\text{Nb}_2\text{O}_5\text{:Zn:Er}$ precursor		Weight percent in the $\text{LiNbO}_3\text{:Zn:Er}$ growth charge	
Zn	Er	Zn	Er
2.70	1.069	2.48	0.98

Table 2. Zinc and erbium concentrations in the $\text{LiNbO}_3\text{:Zn:Er}$ crystals

Crystal	Portion	wt % Zn	wt % Er
1	Cone	1.66	0.77
	Tail end	1.68	0.78
2	Cone	1.7	0.85
	Tail end	1.68	0.82
3	Cone	1.51	0.78
	Tail end	1.55	0.76

For Czochralski growth of zinc–erbium codoped lithium niobate single crystals, we prepared a single-phase $\text{LiNbO}_3\text{:Zn:Er}$ growth charge (Table 1). Chemical analysis data showed that the percentages of niobium (62.26 wt %) and lithium (4.38 wt %) in it corresponded to the congruently melting composition of lithium niobate. The growth charge contained the following cation impurities (wt %): Mg, Mn, Pb, Ni, Sn,



Fig. 2. Appearance of a $\text{LiNbO}_3\text{:Zn(2.48 wt \%):Er(0.98 wt \%)}$ crystal.

Co, Mo, Cu, V, Cr, Ti, Fe, Al, Zr, $<2 \times 10^{-4}$; Ca, Si, $<1 \times 10^{-3}$; Ta, $<1 \times 10^{-2}$. This allowed it to be used for the growth of doped lithium niobate crystals. Fluorine concentration was below the detection limit of the analytical technique used ($<1 \times 10^{-3}$ wt %).

One of the $\text{LiNbO}_3\text{:Zn:Er}$ single crystals grown by us (Fig. 2), 32 mm in diameter, with a 34-mm-long cylindrical body, weighing 128.3 g, was prepared using a homogeneously doped granulated $\text{LiNbO}_3\text{:Zn:Er}$ growth charge. The dopant concentrations in the $\text{LiNbO}_3\text{:Zn:Er}$ growth charge and, accordingly, in the starting melt were 2.48 wt % Zn and 0.98 wt % Er (Table 1). The other two $\text{LiNbO}_3\text{:Zn:Er}$ crystals, 32 and 30 mm in diameter, with a 38- and 40-mm-long cylindrical body, weighing 123.7 and 129.3 g, respectively, were grown by adding a nominally pure LiNbO_3 lithium niobate growth charge to the melt left after the preceding $\text{LiNbO}_3\text{:Zn:Er}$ crystal growth run, that is, by sequentially diluting the starting melt. In this process, no more than 8 wt % of the melt was used for the growth of each $\text{LiNbO}_3\text{:Zn:Er}$ crystal.

Table 2 presents data on the percentages of Zn and Er in the cone and tail end of the $\text{LiNbO}_3\text{:Zn:Er}$ crystals grown by us. The percentages of Zn and Er in the $\text{LiNbO}_3\text{:Zn:Er}$ crystals are considerably lower than the dopant concentrations in the $\text{LiNbO}_3\text{:Zn:Er}$ growth charge and, accordingly, in the starting melt (Tables 1, 2). To evaluate a melt–crystal system, use is commonly made of the effective distribution coefficient K_d (the ratio of the impurity concentration in the crystal in the first instance of crystal growth to the impurity concentration in the melt) and the parameter ΔC , which characterizes the chemical homogeneity of the crystal (dopant concentration difference between the cone and tail end of the crystal). The effective distribution coefficient K_d in the melt–crystal system under consideration is noticeably less than unity for both zinc and erbium (Tables 1, 2). At the same time, the $\text{LiNbO}_3\text{:Zn:Er}$ single crystals have rather uniform dopant distributions along their length (Table 2).

Some fundamental aspects of crystallization processes in the growth of heavily doped lithium niobate crystals were analyzed in previous reports [27, 28]. Whereas the K_d of heavily doped LiNbO_3 crystals is a function of the electronic structure of the dopant, the situation with the parameter ΔC is not so unambiguous. The parameter ΔC of all the $\text{LiNbO}_3\text{:Zn:Er}$ crystals studied by us is rather small, comparable to the uncertainty of the method used to evaluate impurity concentration (Table 2). This points to a high uniformity of the impurity concentration distribution in the crystal growth direction, with K_d noticeably less than unity.

This finding can be accounted for as follows: As a result of doping, the composition of the lithium niobate melt is no longer congruent. This means, in particular, that the spectrum of variations of ionic com-

plexes in the melt in structure and components considerably increases. The melt is captured in a limited zone with a constant temperature near the solid–liquid interface. Therefore, those ionic complexes will crystallize for which this temperature corresponds to their solidus (T_{s1}), clearly, with allowance for some supercooling. As some of the melt is consumed, in the rest of the melt, with $K_d < 1$, the zinc and erbium concentrations increase and, accordingly, the relationship between the concentrations of various ionic complexes varies. As a result, the fraction of the complexes for which T_{s1} is the solidus temperature varies, becoming smaller. This will continue until the system will reach some critical state in which the concentration of complexes with a solidus temperature T_{s1} will be insufficient for crystal growth at a constant impurity concentration. This limits the fraction of the melt that can be solidified to form a chemically homogeneous crystal. In our case, chemically homogeneous $\text{LiNbO}_3\text{:Zn:Er}$ crystals can be obtained if no more than 8 wt % of the melt solidifies. After the described critical state is reached, the system can exhibit different behaviors: from a considerable variation in the impurity concentration in the crystal along its growth direction to cellular growth and crystallization of a phase with a different composition [27, 28].

The conditions needed for such a critical state to be reached and, therefore, the size of a crystal with a constant impurity concentration throughout are influenced by many factors. They include the melt composition, the thermodynamics of the starting components (which are graphically represented by the phase diagram of the system), the structure of the melt (consisting of ionic complexes with different thermodynamic and kinetic characteristics), and even the engineering performance of the growth control and monitoring system [27, 28]. It certainly follows from the above reasoning that doped lithium niobate crystals with a uniform dopant distribution over their bulk can only be grown by the Czochralski technique in the case of solidification of a certain fraction of the melt [27, 28].

The higher zinc and erbium concentrations in crystal 2 (Table 2) are attributable, one the one hand, to a possible increase in K_d with decreasing dopant concentrations in the melt (after the addition of a nominally pure LiNbO_3 growth charge) [28, 29]. On the other hand, the addition of a nominally pure LiNbO_3 growth charge after the growth of crystal 1 to the melt obtained from a homogeneously doped growth charge certainly leads to changes in the structure of the ionic complexes. Note that, in the case of crystallization of such complexes, the impurity distribution coefficient K_d can in general exceed that of the complexes with a solidus temperature T_{s1} , which ensure the growth of crystal 1 as a result of the solidification of the starting melt.

Evaluation of the optical quality of the $\text{LiNbO}_3\text{:Zn:Er}$ single crystals from the number of scattering centers asso-

ciated with the structural defects and internal stress produced during the growth process and subsequent technological processing or due to the presence of cation impurities showed that there were no extended optical defects, nor did we detect any microscopic or mesoscopic defects. Continuous laser beam scanning also did not detect any optical defects anywhere in the bulk of the crystals under investigation.

To ascertain whether the crystals were in a single-domain state, we used a piezoacoustic method [22]. Characteristically, z -oriented lithium niobate single crystals have one main and one side electroacoustic resonance peaks. The amplitude–frequency response (AFR) curves of the crystals under study (Fig. 3) demonstrate that, in all cases, the height of the main resonance peak is about nine times the background. The curves of crystals 1, 2, and 3 have the main peak (main resonance) at frequencies of 163.5, 163.9, and 163.5 kHz, respectively. At the same time, the curve of crystal 1 (Fig. 3a) has three secondary peaks, at frequencies of 56.0, 81.1, and 112.5 kHz; the curve of crystal 2 (Fig. 3b) has two side peaks, at frequencies 82.7 and 116.8 kHz; and that of crystal 3 (Fig. 3c) has three side peaks, at frequencies of 57.8, 83.2, and 117.0 kHz. The results obtained by the piezoacoustic method indicate that, as a result of the transition to a single-domain state, the crystals reached a rather high degree of unipolarity. At the same time, the presence of two or three rather strong secondary resonances in their AFR curves suggests that the crystals have a residual domain structure.

To confirm this fact, we studied the static piezoelectric effect in the crystals. In accordance with a technique described previously [22], we plotted the polarization charge Q_p against force F (Fig. 4) and used these data to calculate the piezoelectric modulus component d_{333} of each crystal: $d_{333}^{(1)} = 6.15 \times 10^{-12}$ C/N, $d_{333}^{(2)} = 2.72 \times 10^{-12}$ C/N, and $d_{333}^{(3)} = 2.7 \times 10^{-12}$ C/N. For comparison, Fig. 4 presents Q_p measurement results for the single crystal 1 before transition into a single-domain state (crystal 4). The calculated piezoelectric modulus component in this case is $d_{333} = 0.85 \times 10^{-12}$ C/N.

In the case of single-domain lithium niobate crystals, the piezoelectric modulus (d_0)₃₃₃ is known to lie in the range $(8–12) \times 10^{-12}$ C/N. It is seen that the piezoelectric modulus components of the crystals under investigation fall beyond this range. Thus, the data obtained in this study are consistent with the AFR measurement results and suggest that the crystals undergo an only partial transition to a single-domain state. The above leads us to conclude that previously developed standard procedures for converting doubly doped (for example, Zn–Mg codoped) lithium niobate crystals into a single-domain state are unsuitable in the case of codoping with zinc and erbium. To reach a higher conversion of $\text{LiNbO}_3\text{:Zn:Er}$ crystals into a

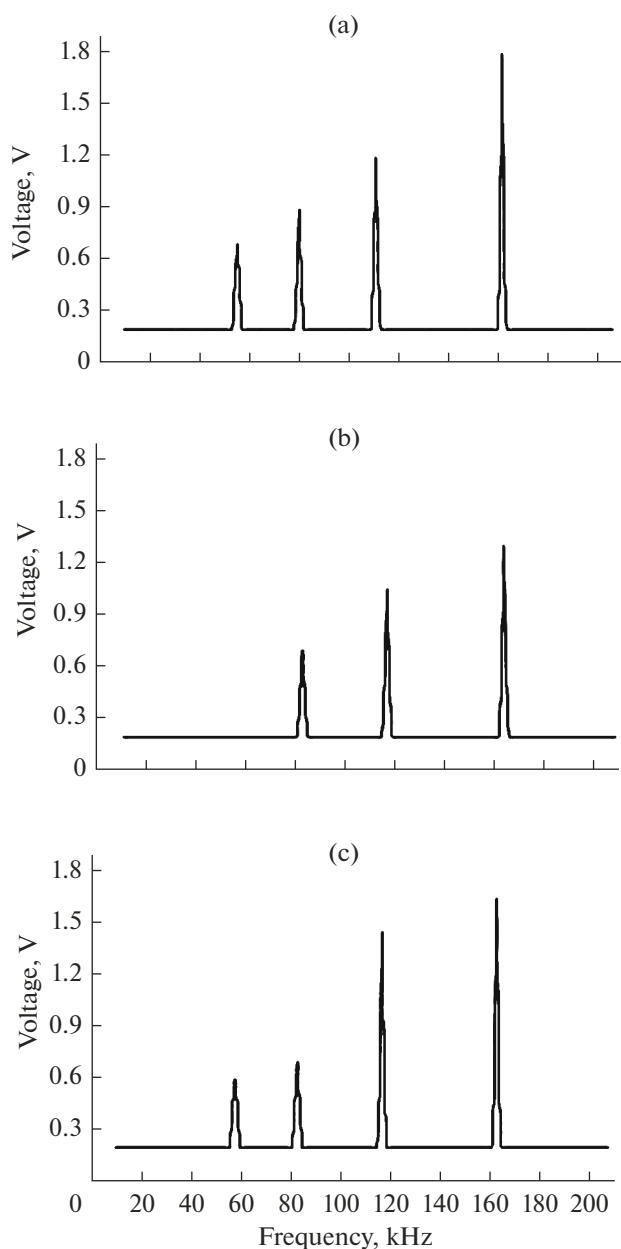


Fig. 3. AFR curves of the low-frequency part of the spectrum of the lithium niobate crystals under study: crystals (a) 1, (b) 2, and (c) 3.

single-domain state, the procedure for conversion into a single-domain state should be modified.

Figure 5 illustrates how PILS patterns of the $\text{LiNbO}_3\text{:Zn:Er}$ crystals vary with time. The appearance of the speckle structure of the PILS indicatrix is characteristic of lithium niobate crystals. At the same time, the speckle structures of PILS in crystals grown by different techniques and differing in composition have their own fine features, which can be used to study the structure of the crystals and assess their micro- and macroscopic homogeneity. It is seen from

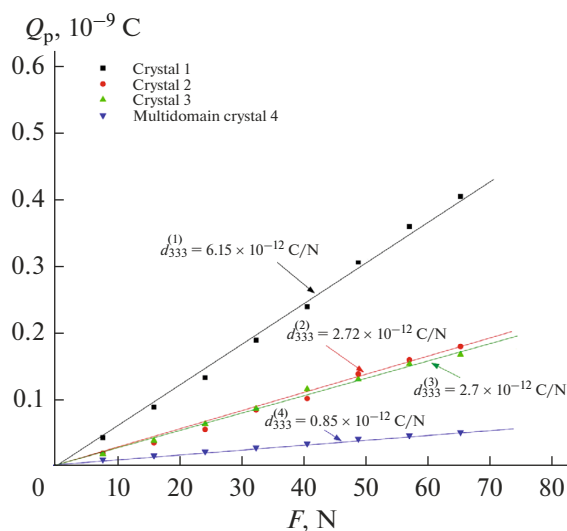


Fig. 4. Q_p as a function of F for crystals 1–3 after conversion to a single-domain state and for the multidomain crystal 4.

Fig. 5 that, even after exposure to 160-mW laser light for 6 min, there is no photorefractive response, the PILS indicatrix does not open, and we observe only scattering by static structural defects. The results obtained by us suggest that the lithium niobate crystals under study are promising as nonlinear optical materials with a weak photorefractive effect and weak PILS, that is, with an insignificant laser beam distortion.

The optical quality of the grown crystals was evaluated using laser conoscopy, a clear and affordable method providing information about the structure, optical properties, and orientation of crystals and the presence of various defects in them [24, 31].

We obtained conoscopic patterns of the crystals under excitation by the MLL-100 laser beam at a low (1 mW) and a high (90 mW) incident light power. The conoscopic patterns obtained under excitation at 1-mW power characterize the structural perfection of the crystal in the absence of a photorefractive effect. The conoscopic patterns obtained under laser excitation at 90-mW power characterize both the intrinsic defects in the crystal (determined by its composition and growth conditions) and defects produced by laser light. Since the $\text{LiNbO}_3\text{:Zn:Er}$ crystals studied by us exhibited no photorefractive effect, their conoscopic patterns obtained at the increased laser output power had no additional anomalies (Figs. 6, 7). Figures 6 and 7 show conoscopic patterns of 1- and 3-mm-thick plates at an incident light power of 90 mW.

The results obtained by laser scanning over the plane of the input face of the $\text{LiNbO}_3\text{:Zn:Er}$ crystals studied by us demonstrate that there are two types of conoscopic patterns, corresponding to uniaxial crystals (Figs. 6a, 6c, 6e, 7a, 7c, 7e) and crystals with an anomalous biaxiality (Figs. 6b, 6d, 6f, 7b, 7d, 7f). The

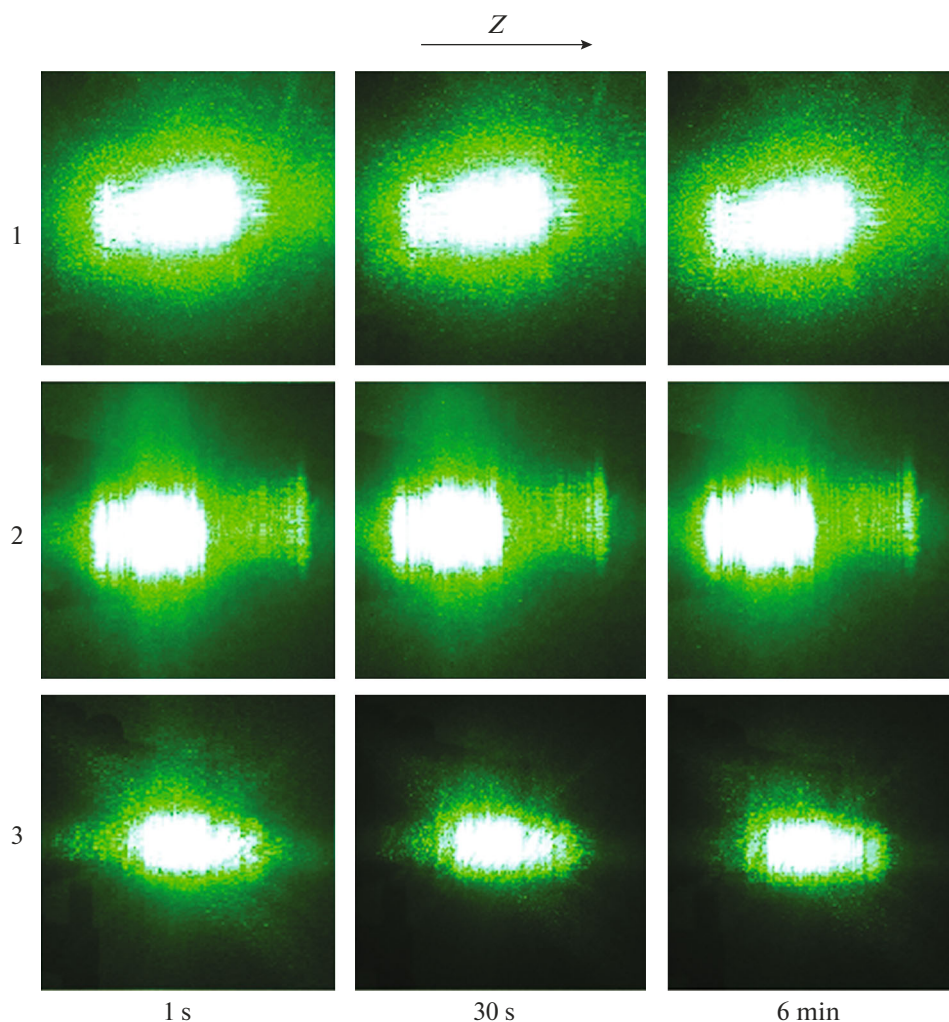


Fig. 5. PLS patterns of the $\text{LiNbO}_3\text{:Zn:Er}$ crystals 1–3 after exposure to laser light for 1 s, 30 s, and 6 min ($\lambda = 532 \text{ nm}$, $P = 160 \text{ mW}$).

conoscopic patterns in Figs. 6a, 6c, 6e, 7a, 7c, and 7e have circular symmetry, with the black “Maltese cross” remaining continuous in the center of the field of view and with isochromes in the form of concentric circles having their center at the point of outcrop of the optic axis. It is this appearance of conoscopic patterns which points to optical homogeneity and good optical quality of the samples. The conoscopic patterns in Figs. 6b, 6d, 6f, 7b, 7d, and 7f have slight signs of an anomalous optical biaxiality, which is responsible for the distortion in the center of the black “Maltese cross” in the form of bleaching and an outward shift of parts of the cross in the direction corresponding to the direction of distortion of the optical indicatrix of the crystal. The isochromes acquire slight ellipticity, retaining a regular geometric shape. It should be noted that the signs of slight optical biaxiality become stronger in going from crystal 1 to crystal 3, which is best seen in the conoscopic patterns of the 3-mm-thick plates (Figs. 7b, 7d, 7f).

Thus, the present results demonstrate that the $\text{LiNbO}_3\text{:Zn:Er}$ crystals studied by us have no photorefractive response and that exposure to 160-mW laser light does not cause their PLS indicatrix to open. According to laser conoscopy results, the crystals have a rather good optical quality. The slight signs of anomalous optical biaxiality present in the conoscopic patterns of all the crystals are attributable to cross-sectional composition fluctuations, detectable when a laser beam propagates through the bulk of a crystalline sample.

CONCLUSIONS

We have developed a process for the preparation of a $\text{Nb}_2\text{O}_5\text{:Zn:Er}$ precursor with tailored composition for the synthesis of a $\text{LiNbO}_3\text{:Zn:Er}$ growth charge containing 2.48 wt % Zn and 0.98 wt % Er. The growth charge has been shown to be single-phase and satisfy relevant technical specifications in terms of regulated

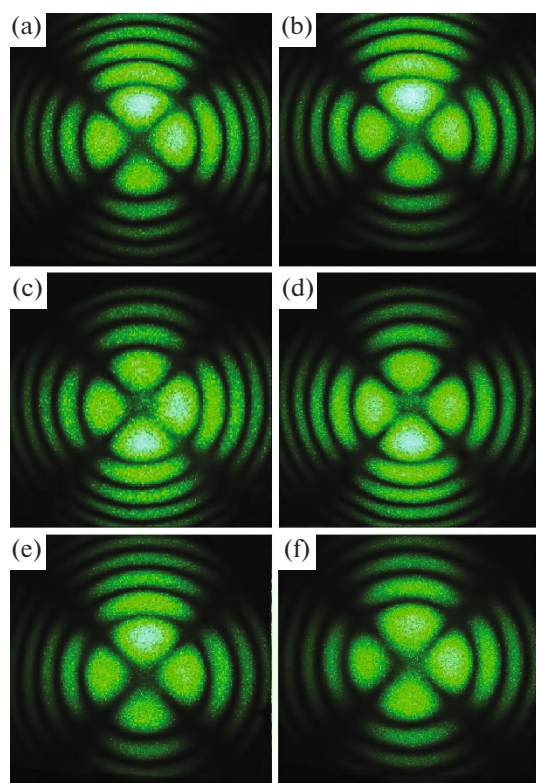


Fig. 6. Conoscopic patterns of the $\text{LiNbO}_3\text{:Zn:Er}$ crystals (1-mm-thick plates): (a, b) crystal 1, (c, d) crystal 2, (e, f) crystal 3 ($\lambda = 532 \text{ nm}$, $P = 90 \text{ mW}$).

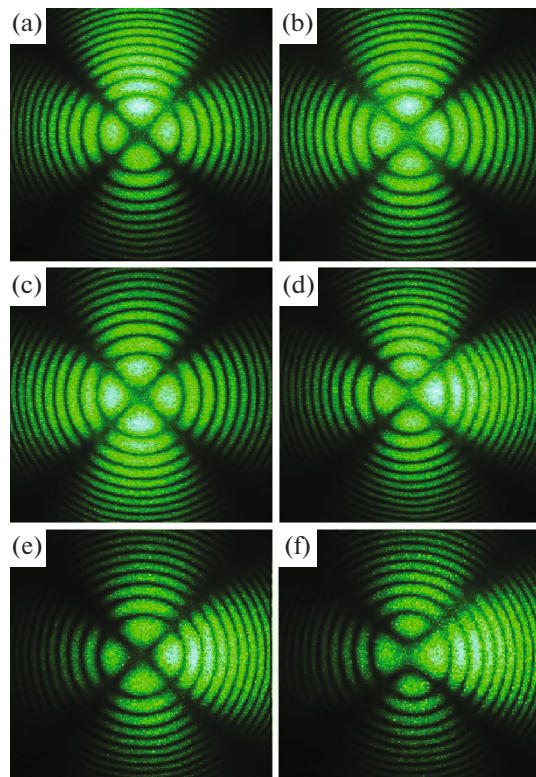


Fig. 7. Conoscopic patterns of the $\text{LiNbO}_3\text{:Zn:Er}$ crystals (3-mm-thick plates): (a, b) crystal 1, (c, d) crystal 2, (e, f) crystal 3 ($\lambda = 532 \text{ nm}$, $P = 90 \text{ mW}$).

impurities, which makes it possible to use it for Czochralski growth of lithium niobate crystals.

Using high-speed evaluation of the optical quality of the $\text{LiNbO}_3\text{:Zn:Er}$ crystals grown using the synthesized charge and diluting the melt with an undoped LiNbO_3 growth charge, we have demonstrated that the crystals are free of microscopic defects. The piezoelectric modulus of the grown $\text{LiNbO}_3\text{:Zn:Er}$ crystals points to an incomplete transition to a single-domain state, suggesting that the procedure for converting such crystals into a single-domain state should be further improved.

Results obtained by assessing optical characteristics of the $\text{LiNbO}_3\text{:Zn:Er}$ crystals clearly demonstrate that they have high optical quality.

REFERENCES

1. Lines, M.E. and Glass, A.M., *Principles and Applications of Ferroelectrics and Related Materials*, Oxford: Clarendon, 1977.
2. Kuz'minov, Yu.S., *Elektroopticheskie i nelineino-opticheskie kristally niobata litiya* (Electro-Optic and Nonlinear Optical Lithium Niobate Crystals), Moscow: Nauka, 1987.
3. Volk, T. and Wohleke, M., *Lithium Niobate. Defects, Photorefraction and Ferroelectric Switching*, Berlin: Springer, 2008.
4. Sidorov, N.V., Volk, T.R., Mavrin, B.N., and Kalinikov, V.T., *Niobat litiya: defekty, fotorefraktsiya, kolebatel'nyi spektr, polyaritony* (Lithium Niobate: Defects, Photorefractive Properties, Vibrational Spectrum, and Polaritons), Moscow: Nauka, 2003.
5. Stoffel, M., Rinnert, H., Kokanyan, E., Demirkhanyan, G., Demirkhanyan, H., and Aillerie, M., Green up-converted luminescence in $(\text{Er}^{3+}\text{-Yb}^{3+})$ co-doped LiNbO_3 crystals, *Opt. Mater.*, 2016, vol. 57, pp. 79–84. <https://doi.org/10.1016/j.optmat.2016.04.013>
6. Munoz, I.C., Landavazo, M.A., Brown, F., Cruz-Zaragoz, E., Alvarez-Montano, V.E., Meléndrez-Amavizca, R., Gil-Tolano, I., and Tánori-Córdova, J., Synthesis and thermoluminescence of erbium-activated lithium niobate, *Appl. Radiat. Isot.*, 2018, vol. 142, pp. 64–70. <https://doi.org/10.1016/j.apradiso.2018.09.020>
7. Fischer, C., Wöhlecke, M., Volk, T., and Rubinina, N., Influence of the damage resistant impurities Zn and Mg on the UV-excited luminescence in LiNbO_3 , *Phys. Status Solidi A*, 1993, vol. 137, pp. 247–252.
8. Maksimenko, V.A., Syui, A.V., and Karpets, Yu.M., *Fotoindutsirovannyye protsessy v kristallakh niobata litiya* (Photoinduced Processes in Lithium Niobate Crystals), Moscow: Fizmatlit, 2008.
9. Tu, X., Wang, S., Xiong, K., Chen, Y., Zheng, Y., and Shi, E., Growth and properties of Pr^{3+} doped LiNbO_3 crystal with Mg^{2+} incorporation: a potential material for quasi-parametric chirped pulse amplification, *Opt. Mater.*, 2020, vol. 105, paper 109893. <https://doi.org/10.1016/j.optmat.2020.109893>
10. Masloboeva, S.M., Biryukova, I.V., Palatnikov, M.N., and Teplyakova, N.A., Magnesium-and-zinc-doped

- lithium niobate crystals: preparation and characterization, *Russ. J. Inorg. Chem.*, 2020, vol. 65, no. 6, pp. 924–931.
<https://doi.org/10.1134/S0036023620060108>
11. Mkhitarian, N., Zaraket, J., Kokanyan, N., Kokanyan, E., and Aillerie, M., Electro-optic properties of singly and doubly doped lithium niobate crystal by rare earth elements for optoelectronic and laser applications, *Eur. Phys. J.: Appl. Phys.*, 2019, vol. 85, paper 30502.
<https://doi.org/10.1051/epjap/2019180317>
 12. Xiaolong, Y., Guanfeng, X., Heping, L., Jianguo, Z., and Xiu, W., Optical absorption edge of Mg + Zn:LiNbO₃, *Cryst. Res. Technol.*, 1996, vol. 4, pp. 521–527.
 13. Zhang, T., Wang, B., Ling, F.R., Fang, Sh.Q., and Xu, Y.H., Growth and optical property of Mg, Fe codoped near-stoichiometric LiNbO₃ crystal, *Mater. Chem. Phys.*, 2004, vol. 83, pp. 350–353.
 14. Fan, Y., Xu, C., Xia, S., Guan, C., Cao, L., He, Q., and Jin, G., Growth and spectroscopic characterization of Zr:Fe:LiNbO₃ crystals with various Li/Nb ratios, *J. Cryst. Growth*, 2010, vol. 312, pp. 1875–1878.
<https://doi.org/10.1016/j.jcrysgro.2010.03.001>
 15. Stroganova, E.V., Galutskii, V.V., Nalbantov, N.N., and Kozin, A.S., Spectroscopic and luminescent characteristics of gradient-doped LiNbO₃ crystals with Yb³⁺ and Er³⁺ concentration profiles, *Aviometriya*, 2017, vol. 53, no. 1, pp. 94–99.
<https://doi.org/10.15372/AUT20170111>
 16. Zhen, X., Wang, R., Zheng, W., Zhao, L., and Xu Yu, Optical properties of Zn,Er-codoped Li-rich LiNbO₃ crystal, *Proc. SPIE. Optoelectron., Mater., Devices Commun.*, 2001, vol. 4580, pp. 548–550.
<https://doi.org/10.1117/12.445013>
 17. Pernas, P.L., Hernandez, M.J., Ruiz, E., Cantelar, E., Nevado, R., Morant, C., Lifante, G., and Cusso, F., Zn-vapor diffused Er:Yb:LiNbO₃ channel waveguides fabricated by means of SiO electron cyclotron resonance plasma deposition, *Appl. Surf. Sci.*, 2000, vol. 161, pp. 123–134.
[https://doi.org/10.1016/S0169-4332\(00\)00147-1](https://doi.org/10.1016/S0169-4332(00)00147-1)
 18. Palatnikov, M.N., Sidorov, N.V., and Kalinnikov, V.T., *Segnetoelektricheskie tverdye rastvory na osnove oksidnykh soedinenii niobiya i tantala: sintez, issledovanie strukturnogo uporyadocheniya i fizicheskikh kharakteristik* (Ferroelectric Solid Solutions Based on Niobium and Tantalum Oxide Compounds: Synthesis, Structural Ordering, and Physical Characterization), St. Petersburg: Nauka, 2002, 2nd ed.
 19. Masloboeva, S.M., Palatnikov, M.N., Arutyunyan, L.G., and Ivanenko, D.V., Methods for the preparation of a doped lithium niobate growth charge, *Izv. S.-Peterburg. Gos. Tekhnol. Inst. (Tekh. Univ.)*, 2017, no. 38 (64), pp. 34–43.
 20. Masloboeva, S.M., Kalinnikov, V.T., Zalkind, O.A., Kadyrova, G.I., and Kuznetsov, V.Ya., Preparation of Zn²⁺-doped niobium pentoxide for lithium niobate crystal growth, *Tsvetn. Met.*, 2012, no. 5, pp. 89–92.
 21. Palatnikov, M.N., Sidorov, N.V., Makarova, O.V., and Biryukova, I.V., *Fundamental'nye aspekty tekhnologii sil'no legirovannykh kristallov niobata litiya* (Fundamental Aspects of the Technology of Heavily Doped Lithium Niobate Crystals), Apatity: Kol'sk. Nauchn. Tsentr Ross. Akad. Nauk, 2017.
 22. Masloboeva, S.M., Efremov, I.N., Biryukova, I.V., and Palatnikov, M.N., Growth and characterization of a boron-doped lithium niobate single crystals, *Inorg. Mater.*, 2020, vol. 56, no. 11, pp. 1147–1152.
<https://doi.org/10.1134/S0020168520110072>
 23. Pikoul, O.Yu., Alekseeva, L.V., Povkh, I.V., Stroganov, V.I., Rudoi, K.A., Tolstov, E.V., and Krishtop, V.V., Distinctive features of an optical system for producing large conoscopic patterns, *Izv. Vyssh. Uchebn. Zaved., Pribo-rostr.*, 2004, vol. 47, no. 12, pp. 53–55.
 24. Pikoul, O., Determination of the optical sign of a crystal by a conoscopic method, *J. Appl. Crystallogr.*, 2010, vol. 43, pp. 955–958.
<https://doi.org/10.1107/S0021889810022375>
 25. Pollard, A.J., Note on the system niobium oxide–zinc oxide, *J. Am. Ceram. Soc.*, 1961, vol. 44, no. 12, pp. 630–635.
<https://doi.org/10.1111/j.1151-2916.1961.tb11672.x>
 26. Hsu, R., Maslen, E.N., Boulay, D., and Ishizawa, N., Synchrotron X-ray studies of LiNbO₃ and LiTaO₃, *Acta Crystallogr., Sect. B: Struct. Sci.*, 1997, vol. 53, pp. 420–428.
<https://doi.org/10.1107/S010876819600777X>
 27. Makarova, O.V., Palatnikov, M.N., Biryukova, I.V., and Sidorov, N.V., Impact of a dopant impurity electronic structure on physical properties, defect structure and features of lithium niobate doping technology, *Tech. Phys.*, 2019, vol. 64, no. 12, pp. 1872–1878.
<https://doi.org/10.1134/S1063784219120168>
 28. Palatnikov, M.N., Sidorov, N.V., Manukovskaya, D.V., Makarova, O.V., and Aleshina, L.A., Concentration threshold effect on properties of zinc-doped lithium niobate crystals, *J. Am. Ceram. Soc.*, 2017, vol. 100, no. 8, pp. 3703–3711.
<https://doi.org/10.1111/jace.14851>
 29. Palatnikov, M.N., Biryukova, I.V., Sidorov, N.V., Denisov, A.V., Kalinnikov, V.T., Smith, P.G.R., and Shur, V.Ya., Growth and concentration dependencies of rare-earth doped lithium niobate single crystals, *J. Cryst. Growth*, 2006, vol. 291, pp. 390–397.
 30. Blistanov, A.A., Bondarenko, V.S., Chkalova, V.V., et al., *Akusticheskie kristally. Spravochnik* (Acoustic Crystals: A Handbook), Shaskol'skaya, M.P., Ed., Moscow: Nauka, 1982.
 31. Rudoi, K.A., Nabatov, B.V., Stroganov, V.I., Konstantinova, A.F., Alekseeva, L.V., Evdishchenko, E.A., and Kidyarov, B.I., Conoscopic figures of optically active uniaxial crystals, *Crystallogr. Rep.*, 2003, vol. 48, no. 2, pp. 300–304.

Translated by O. Tsarev